Effect of Settlement Rate and Geogrid Reinforcement on the DeformationBehaviour of Soil Barriers of Landfill Covers: Centrifuge Study

S. Rajesh[1] and B.V.S. Viswanadham[2]
[1]*Department of Civil Engineering, Indian Institute of Technology Kanpur, India*
[2]*Department of Civil Engineering, Indian Institute of Technology Bombay, India*
[1]*E-mail*: *hsrajesh@iitk.ac.in*
[2]*E-mail*: *viswam@civil.iitb.ac.in*

ABSTRACT: The objective of this paper is to examine the influence of settlement rate and geogrid reinforcement on the deformation behaviour of soil barriers of landfill covers subjected to differential settlements. A series of centrifuge tests were performed on soil barriers at 40 gravities. Two different settlement rates were induced using motor-based differential settlement simulator designed for a high gravity environment. Centrifuge tests on a 1.2 m thick unreinforced soil barrier subjected to two different settlement rates without provision of any overburden pressure was found to experience identical deformation profiles and cracking pattern. A slight delay in the occurrence of crack initiation and an increase in the strain at crack initiation was noticed when the soil barrier was tested at slow settlement rate. An increase in the limiting distortion level from 0.044 to 0.069 was noticed when the unreinforced soil barrier was subjected to an overburden pressure equivalent to that of cover system. When the soil barrier was reinforced with a geogrid layer without any overburden pressure, the limiting distortion level was increased from 0.044 to 0.064. An increase in the maximum mobilized tensile load of model geogrid from 77 kN/m to 120 kN/m was observed with the provision of overburden pressureequivalent to that of cover system.

1. INTRODUCTION

Waste containment systems of Municipal Solid Waste (MSW) landfills are known to undergo significant differential settlements due to biodegradation of waste (Duplancic, 1990; Daniel, 1993). In general, the composition of MSW was found to have biodegradable component (mainly food waste, garden waste, tree leaves, market waste, other putriscible matter etc.), bio-resistant component (mainly leather, rubber, plastic, synthetic material etc.) and inert material component (like construction debris, cinder, tiles, ash, dust, etc.). Since the MSW is highly heterogeneous material and can settle either due to biodegradation of waste, or by its own weight or by overlying pressure applied above the barrier, occurrence of differential settlements of varying order, within the landfill area are common. Koerner and Daniel (1997) reported that for a conventional / passive landfill, a total settlement of 10 to 20 % of the original height of the fill may occur in less than 30 years, whereas, in leachate recirculation / bioreactor / active landfills, the same amount of settlement may happen in less than 15 years. Benson et al. (2007) found that over 2.7 years, waste in a bioreactor landfill site settled by 22 – 25% (i.e., total settlement / initial thickness of waste), while a conventional landfill settled less than 5% for the identical duration. Moreover, it was also found that average rate of settlement for the bioreactor landfill was approximately 14% during the first 16 months, and about 6% during the latter 18 months but in the conventional landfill, waste settled at a relatively uniform rate of approximately 1.5% per year. It can be noticed from the review of literature that settlement rates in bioreactor landfills are found to be larger than those of conventional landfills for a given period of time. In addition, due to non-uniform recirculation of leachate through injection wells, the occurrence of the differential settlements is quite natural and more pronounced. Interestingly, settlement rate was found to vary depending on the design philosophy.

Qian et al. (2002) categorized differential settlements of landfill covers as large craters to localized depressions. Large craters having a distortion level of 0.167 resulted in a maximum strain of about 1.8 % in landfill covers. In comparison, a typical local depression having a distortion level of 0.27 resulted in a maximum strain of about 4.5 %. The distortion level is defined as the ratio of central settlement at any stage of deformation to the influence length within which differential settlements are induced. The excessive differential settlements can result in the development of tension cracks in the soil barrier or tearing of geomembrane or displacement of bentonite from GCL, near the zone of sharp curvatures there by resulting in loss of integrity of the whole cover system. This led several researchers to work towards developing ideal barrier materials which can resist higher distortion level; and to understand the deformation behavior of various barrier materials against differential settlement. Compacted clay can be used effectively as a hydraulic barrier because of clay's low permeability, and hence such barriers are widely used wherever clay soils are abundantly available (Gourc et al., 2010). Jessberger and Stone (1991), Viswanadham and Mahesh (2002), Viswanadham and Rajesh (2009) presented results of centrifuge tests on the deformation behavior of clay based soil barriers and found that commonly adopted thicknesses of the soil barrier (0.6 m to 1.2 m) tend to experience severe cracking and lose their integrity at low distortion level itself. Cracking of the soil barrier may be primarily due to the low tensile strength of the soil barrier material. Several researchers tried different methods for improving the deformation behavior of clay-based soil barriers subjected to differential settlements, such as blending high plasticity material like bentonite to the locally available soil which is used for preparing soil barrier, providing double cover system (i.e., providing geomembrane below soil barrier), mixing discrete fibers to the soil barrier material uniformly or placing geogrid within the soil barrier (Viswanadham et al., 2011; ViswanadhamandJessberger, 2005). However, the knowledge pertaining to the effect of settlement rate and geogrid reinforcement on the deformation behaviour of clay-based soil barriers is limited. Hence, this forms research interest and motivation behind the present study.

2. CENTRIFUGE TEST PROGRAM AND TESTING PROCEDURE

The concept of small-scale model testing to study the physical phenomena is widespread in the engineering field. However, in the geotechnical field, since the stress levels in a small laboratory model are not the same as the stress levels in the full-scale prototype, the use of small-scale modelling may not simulate the exact field conditions. However, this can be addressed by subjecting a small-scale physical model to high gravities by rotating about a vertical axis in a horizontal plane(Schofield, 1980). A geotechnical centrifuge can induce centripetal accelerations, which are many times greater than the earth's gravitational acceleration on a small-scale model, so as to make the identical stress conditions in the model at homologues points as that of in the prototype. It is

necessary to develop scaling relationships appropriately to replicate a prototype response in a small-scale model which link the model behavior to that of the prototype. Scaling laws can be derived by making use of dimensional analysis or from a consideration of the governing differential equations. Centrifuge scaling factors and errors due to high acceleration field have been described elsewhere extensively (Schofield, 1980). Application of centrifuge modeling technique to the present study is relevant because the loss of integrity of soil barriers is highly influenced by the presence of prototype stress conditions. The centrifuge tests reported in the present study were performed using a 4.5 m radius large beam centrifuge facility at Indian Institute of Technology Bombay (IIT Bombay) at an acceleration of 40 g. The centrifuge has a swing basket at one end and an adjustable counterweight at the other end. The centrifuge capacity is 2500 g-kN with a maximum payload of 25 kN at 100 g. At higher acceleration of 200 g the allowable payload is 6.25 kN. With the help of an on-board central processing unit, LAN connections and embedded signal conditioning and filter cards, data can be continuously acquired and stored(Rajesh and Viswanadham, 2012).

2.1 Relevant scaling relations for the present study

If an N times acceleration of the Earth's gravity (g) is applied to a material of density ρ, then the vertical stress, $\sigma_v$at depth h_m in the model (subscript 'm' indicates the model) is given by $\sigma_{vm} = \rho N g h_m$. In the prototype, vertical stress$\sigma_{vp}$is given by $\sigma_{vp} = \rho g h_p$. Thus, to have scale factor of stress to be unity, σ_{vm} should be equal to σ_{vp} which makes the height of the model h_m to be $h_m = h_p / N$. Hence, the scale factor (model: prototype) for linear dimensions in 1:N. Since the model is a linear scale representation of the prototype, displacements will also have a scale factor of 1:N. Hence, strains have a scale factor of unity (1:1). The scale factor for the time of consolidation using dimensional analysis was found to be 1: N^2. The settlement rate, S_r is defined as the ratio of settlement over time (a/t). The scale factor for S_r can be derived by substituting scale factors of linear dimension and time related to consolidation process in the expression; which gives a scale factor as N:1. The scale factor for settlement rate suggests that the settlement rate in a centrifuge model is N times higher than that of prototype settlement rate. The nature of induced deformations to the soil barrier can be explained using the parameters like settlement ratio and distortion level. When the horizontal distance from centre of the soil barrier x is zero, the value of settlement is termed as a central settlement a (refer Fig. 1); maximum central settlement induced in the present study is 25 mm (1 m at 40g). Settlement ratio, $a/a_{max}$is defined as the ratio of central settlement at any stage of deformation a to the maximum central settlement a_{max}. Distortion level, a/l is defined as the ratio of central settlement a to the influence length l (which is defined as a distance over which induced settlements cease to zero)within which differential settlements are induced (refer Fig. 1a). In the present study, l = 200 mm (in model dimensions) was used. Scale factors for settlement ratio and distortion level are 1:1. The scaling-down of geosynthetic materials is essential in small-scale physical modelling studies in order to obtain the correct response of a prototype structure. The scaling relationships for modelling geogrid are deduced by considering two basic requirements, namely, (i) scaling of frictional bond behaviour, and (ii) scaling of tensile load-strain behaviour. Scale factors for percentage open area, tensile load of geogrid and secant modulus of geogrid was found to be 1:1, 1:N and 1:N respectively (Viswanadham and König, 2004).

2.2 Model Materials

2.2.1 Soil

In order to model a soil barrier in the laboratory, it is important that it should represent the barrier material properties used in the field. This was achieved by analysing the data from 85 landfills in the USA presented by Benson et al. (1999). Most of the soil barriers are compacted on the wet side of optimum using standard Proctor compaction energy. It was reported that, in most of the landfill sites, soil barriers constructed in the cover system have liquid limit ranging from 30% to 40% and plasticity index ranging from 10% to 20% respectively. In the present study, the soil barrier was modelled in such a way that it represented the above material characteristics. Various blends of commercially available kaolin and naturally available sand were tried to achieve the ideal properties, from which a kaolin-sand mix of 4:1 by dry weight was chosen as the model soil barrier material. The fine sand used for development of the model material in the present study was uniformly graded, and is classified as SP according to the USCS. The maximum and minimum void ratios of the sand are 0.895 and 0.597, respectively, and the corresponding unit weights are 13.57 kN/m^3 and 16.43 kN/m^3.The properties of model soil barrier material are summarized in Table 1.

Table 1 Properties of model soil barrier material

Properties	Values
Specific gravity	2.54
Liquid limit [%]	38
Plasticity index [%]	16
Standard Proctor Compaction:	
Maximum dry unit weight [kN/m^3]	15.9
Optimum moisture content [%]	22
Shear strength parameter (at 5% optimum) (CU triaxial):	
Cohesion,c′ [kPa]	19
Angle of internal friction, ϕ′ [°]	29
Coefficient of permeability [m/s]	0.4 x 10^{-9}

2.2.2 Geogrid

In order to simulate thickness of the soil barrier of 1.2 m; maximum central settlement of 1 m and overburden pressure equivalent to 25 kN/m^2, centrifuge tests were planned to be conducted at 40 gravities (i.e., N = 40). The purpose of selecting the 40 g acceleration level and reason for choosing variation of thickness of the soil barrier and the overburden pressure was explained elsewhere extensively by Viswanadham and Rajesh (2009). Table 2 summarizes the properties of the scaled-down model geogrid along with its projected prototype values corresponding to 40 g and the average range of values of commercially available geogrids. The percentage open area expressed in percentage is the ratio of area formed by grid opening sizes (or aperture sizes) to area formed by grid opening sizes measured up to centre of width of ribsof the model geogrid was found to be in good agreement with the commonly available prototype geogrids. Model geogrid was tested for its wide-width tensile strength, as per ASTM D 4595 (2005). The average value of tensile load corresponding to 2% and 5% strain, ultimate tensile strength and ultimate strain of the model geogrid in machine and cross-machine directions are tabulated in Table 2. It can be noticed that model geogrid used in the present study can represent a relatively stiff prototype biaxial geogrid at 40 g.

2.3 Instrumentation for model geogrid

In the present study, an attempt has been made to measure the mobilized tensile load of the geogrid layer at various ranges of distortion levels using calibrated model geogrid instrumented with miniature foil type strain gauges. Strain gauges of 0.6 mm in length, 0.8 mm in width with a base of 5.3 mm x 1 mm having a nominal resistance of 120Ω, gauge length of 0.6 mm, gauge factor of 2.24 and strain limit of 3% were used. As the width of ribs of scale-down model geogrids are very small, pasting of strain gauges on to ribs will not be possible and even if it is done, the response could be highly localized. Hence, in this study, a 25 mm x 25 mm square portion in the centre of the selected geogrid sample at predetermined locations was filled with 2 mm thick rubber-based backing material. Strain gauges were oriented in such a way that they can only

measure the tensile strain. Two dummy strain gauges for each channel were pasted on to a 6 mm thick Perspex sheet coated with a rubber-based backing material, identical to the one adopted for model geogrids, to facilitate temperature compensation. A custom designed and developed load-based calibration test setup was used to calibrate instrumented model geogrid for measuring the change in resistance, which in-turn can be used to determine mobilized tensile load of geogrid under various magnitudes of applied loads. The obtained calibration factors were used for determining the mobilized tensile load of the geogrid embedded in the soil, while inducing differential settlements in a centrifuge. The detailed explanation covering the selection of backing material, layout of strain gauges, calibration procedure and the calibration charts can be obtained from Rajesh and Viswanadham (2012).

Table 2 Properties of chosen model geogrid material

Properties	Model geogrid	Prototype geogrids (average values)
Percentage openarea [%]	68	60-90
Average area weight [g/m^2]	153.1	-[a]
Average tensile load at 2% strain [kN/m]MD / XD	81(2.02) / 82 (2.06)	
Average tensile load at 5% strain [kN/m]MD / XD	180 (4.51) / 138 (3.45)	75-250[b]
Average ultimate strain [%] MD / XD	18.75 / 22.21	10-18 [c]

-[a] not reported / available; [b] ultimate tensile strength; [c] Both in Machine (MD) and Cross-Machine (XD) directions; model dimensions values are given within the parenthesis.

2.4 Test program

In the present study, the influence of settlement rate, overburden pressure and geogrid reinforcement on the deformation behavior of 1.2 m thick soil barriers at the onset of differential settlements was studied with the help of seven centrifuge tests. Some of the results of these centrifuge model tests were presented in Rajesh and Viswanadham (2009, 2012). The differential settlements were induced at a particular settlement rate in flight (at 40 g) using custom designed motor-based differential settlement simulator (MDSS). The MDSS system works on a simple principle: the rotational movement of the motor shaft is converted to translational movement of the central platform through a screw jack and a series of gears (Rajesh and Viswanadham, 2010). Settlement rates achieved in model dimensions in the present study are 1 mm/min and 0.5 mm/min. Corresponding settlement rates at 40 gravities (s_{rp}) are 36 mm/day and 18 mm/day respectively. The maximum central settlement (a_{max}) induced in all centrifuge tests reported in this paper is 25 mm in model dimension (i.e., 1 m at 40 g). The induced settlement rates and maximum central settlement may not be realistic but to some extent these prototype settlement rates represent excessive settlement near the drains in bioreactor landfills, localized depression or sudden collapse of the waste container, or ground subsidence in waste disposal sites (Qian et al., 2002 and Gourc et al. 2010). The influence of geogrid reinforcement on the deformation behaviour of the soil barrier was examined by placing scale-down instrumented geogrid at one-fourth the thickness of the soil barrier measured from the top surface of the soil barrier (d_g = 0:25d). This location of the geogrid within the soil barrier was chosen because of its effectiveness when compared with other positions (Kuo and Hsu, 2003). Sealing efficiency of the soil barrier at various ranges of distortion level has been studied by placing calculated quantity of water above the soil barrier. This was achieved through data measured with the help of pore pressure transducers placed on the surface of the soil barrier. In MSW landfills, the thickness of the cover soil along with the water drainage layer placed above the soil barrier in the cover system (about 1 to 1.5 m) can generate an overburden pressure of 25 kPa, hence, few centrifuge tests were performed at an overburden pressure of 25 kPa.

Table 3 presents the details of centrifuge tests reported in this paper. In order to showcase the repeatability of the test results (r at the end of test legend indicates repeated test with same boundary conditions), two centrifuge tests were repeated. Each centrifuge test reported was given an identification code. The first letter in the identification code U and G indicates unreinforced soil barrier (URSB) and geogrid reinforced soil barrier (GRSB). Numbers following the letter indicate settlement rate in model dimensions and overburden pressure. For example, case U-1-25 refers to a case where unreinforced soil barrier is subjected to a settlement rate of 1 mm/min and overburden pressure of 25 kPa.

Table 3 Details of centrifuge model tests

Test Legend	*RI*	*d* (m)	S_{rm} (mm/min)	σ_o (kPa)
U-1-0	No	1.2	1	0[a]
U-1-0r[c]	No	1.2	1	0[a]
U-0.5-0	No	1.2	0.5	0[a]
U-0.5-0r[c]	No	1.2	0.5	0[a]
U-1-25	No	1.2	1	25
G-1-0	Yes	1.2[b]	1	0[a]
G-1-25	Yes	1.2[b]	1	25

RI- Reinforcement inclusion; d – thickness of the soil barrier; S_{rm}Settlement rate in model dimensions;σ_o -overburden pressure; [a]water kept above the soil barrier to quantify infiltration; [b]d_g/d =0.25;d_g – location of geogrid from top surface of the soil barrier;[c]tested for repeatability and reproducibility.

2.5 Test procedure

Figure 1 shows the front elevation of the portion of the URSB without any overburden pressure [Fig. 1a] and GRSB with 25 kPa overburden pressure [Fig. 1b] before and after inducing a central settlement of 1 m at 40 g. A 30 mm thick model soil barrier (1.2 m at 40 *g*) was prepared at its wet side of optimum (OMC+5%) and corresponding dry unit weight (14.2 kN/m^3) above pre-saturated and drained coarse and fine layers of sand having 30 mm thickness. The calibrated instrumented model geogrid was placed at d_g distance and then the remaining thickness of the soil barrier was constructed. Discrete markers were embedded on the soil barrier along its cross-section and longitudinal section to capture the deformation pattern and cracking pattern of the soil barrier respectively. The overburden pressure of 25 kPa equivalent to the cover system was applied at 40 gravities, by placing 27 mm thick saturated sand layer and 10 mm high inundated water (prepared at normal gravity). The deformation profiles of the geogrid layer in the case of GRSB can be obtained by series of discrete markers glued on to the instrumented scale-down model geogrid (refer Fig. 1b). At various stages of central settlements and distortion levels, photographs were captured using digital photo camera placed on the front side of the model to view right half of the front elevation of the soil barrier and were later used for image analysis to compute displacement profiles and strain distribution along the top surface of the soil barrier. Various sensors like miniature pore pressure transducers (PPTs), linearly variable differential transformers (LVDT) and strain gauges were used to measure water breakthrough, displacement profiles of the soil barrier and mobilized tensile load of model geogrid respectively.

3. METHOD OF ANALYSIS

The information obtained from various sensors (like PPTs, LVDTs and strain gauges) and digital photographs throughout the centrifuge testing were used to continuously monitor the deformation behavior

of soil barrier under various distortion levels, settlement rates, overburden pressure and geogrid reinforcement. Even though central settlement was induced continuously, for the sake of analysis, performance assessment of the soil barrier is examined for various stages of central settlement ranging from zero to 1 m, in intervals of 0.2 m. The influence of settlement rate and geogrid reinforcement on the deformation behavior of the soil barrier subjected to differential settlement was evaluated with the help of strain distribution, water breakthrough, limiting distortion at the onset of breakthrough and mobilized tensile load of geogrid.

3.1 Computation of total strain

The shape of the deformed soil barrier (i.e., displacement profile of the soil barrier) at various stages of central settlement can be used to determine the magnitude of total strain for respective central settlement using combined bending and elongation method (Tongon et al., 2000). The displacement profiles of the soil barrier can be obtained from the digital image analysis of the discrete markers embedded on the top surface of the soil barrier. The digital photographs captured at various stages of central settlement were used to determine the displacement of the discrete markers with respect to a rectangular grid of permanent markers fixed onto the inner side of the Perspex sheet (Fig.1). The distribution of the strains along the surface of soil barrier was determined using the image analysis software (GRAM++, 2004) with the help of measure co-ordinates of each marker at various stages of central settlement. The measured coordinates of markers are approximated with an exponential equation of the normal distribution to get the displacement profile of the soil layers at various stages of central settlement. Let $w(x)$ is the deformation profile of the soil barrier then total strain and this can be determined by knowing the slope and curvature of the deformation profile of the soil barrier. The total strain experienced by the soil barrier is the summation of elongation strain and bending strain. Elongation strain is the strain due to change in length which can be approximately obtained from $w'(x)$. Bending strain is the strain due to change in curvature which can be computed using $\varepsilon_k(x) = R_{of}\,\kappa(x)d$; where, $\kappa(x)$ is the curvature of the soil barrier along the horizontal distance x, which is equal to $[1/R(x)]$ and is equal to $w''(x)$, second derivative of $w(x)$; and $R(x)$ is the curvature radius of the soil barrier along the horizontal distance x, R_{of} is the neutral layer coefficient which is taken as 0.667, d is the thickness of the soil barrier.

3.2 Computation of Infiltration ratio

The performance of the model soil barrier as an effective hydraulic barrier can be better illustrated through the infiltration of water through the soil barrier. In order to determine infiltration of water, a measured quantity of water (30 mm free-standing water, in model dimensions) was kept above the surface of the soil barrier. The reduction in the volume of the water at any stage of centrifuge testing at the onset of differential settlements can be determined using the change in water levels measured using PPTs (refer Fig. 5). The PPTs are installed at suitable spacing (considering symmetry, only right side of the model) on the top surface of the soil barrier. The volume of water can be determined as the product of the width of the soil barrier and area under measured water profile (i.e., numerical integration). The change in the volume of water at any stage of central settlement can be obtained from the numerical difference between the initial volume of water v_o to the volume of water at the required settlement stage v_a. The infiltration ratio IFR can be determined from the ratio of the change in the volume of water at any stage of central settlement to the initial volume of water.

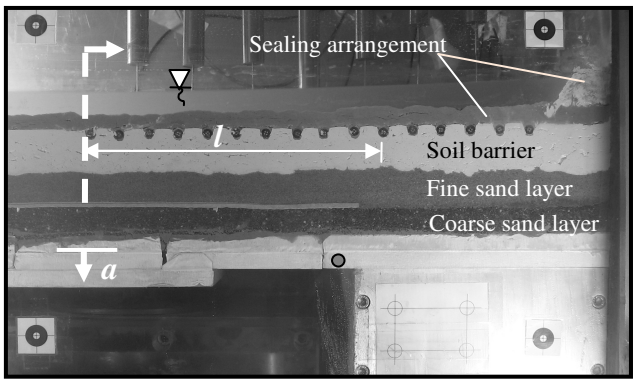

i) at$a$ = 0; a/l = 0

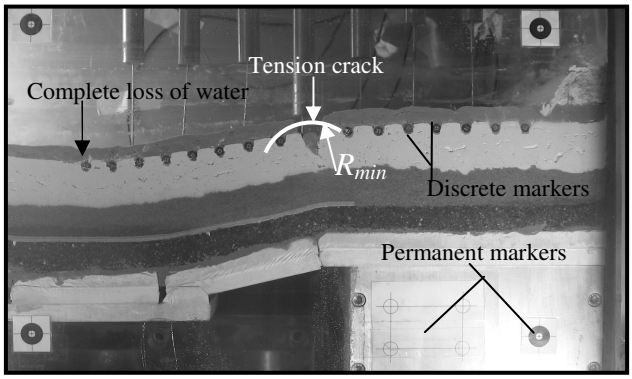

ii) at$a$ = 25 mm (1 m); a/l = 0.125

a) Case: U-1-0 (σ_o = 0 kPa)

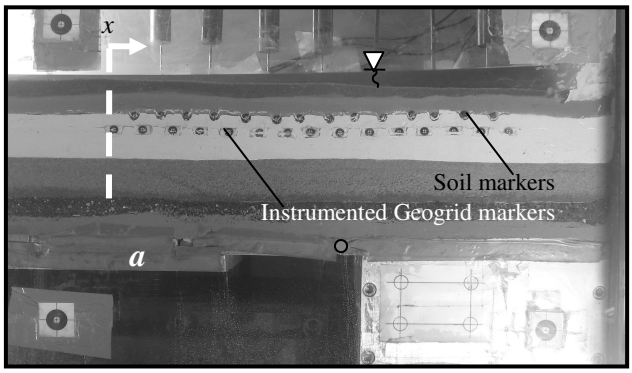

i) Case: U-1-0 (σ_o = 0 kPa)

ii) at$a$ = 25 mm (1 m); a/l = 0.125

b) Case: G-1-25(σ_o = 25 kPa)

Figure 1 Deformation of soil barriers before and after inducing settlement [Cases: U-1-0 and G-1-25]

4.1 Influence of settlement rate and geogrid reinforcement

The influence of settlement rates on the deformation behaviour of soil barrier was studied by performing four centrifuge tests with two settlement rates of 1 mm/min and 0.5 mm/min (in model dimensions). The thickness of the soil barrier was 1.2 m. Centrifuge tests performed in this series are without any overburden pressure. The actual duration of the test in model dimensions for inducing 25 mm central settlement in the centrifuge for model settlement rates (S_{rm}) equivalent to 1 mm/min and 0.5 mm/min, was 25 and 50 minutes respectively; in actual practice, it corresponds to 28 and 56 days respectively.

Table 4 Summary of centrifuge test results

Parameters	U-1-0	U-0.5-0	U-1-25	G-1-0	G-1-25
Type of test	URSB	URSB	URSB	GRSB	GRSB
σ_o [kPa]	0	0	25	0	25
S_{rm} [mm/min]	1	0.5	1	1	1
ε_{max} [%]	3.41	3.69	3.81	3.34	3.76
$(a/l)_{lim}$	0.044	0.033	0.069	0.064	0.125*
d_c [mm]	1200 (30)	1200 (30)	1200 (30)	300 (7.5)	~0.1
w_c [mm]	152 (3.81)	148.8 (3.72)	108 (2.7)	27 (0.68)	~0.3
Max $T_{g(mob)}$ [kN/m]	[a]	[a]	[a]	77 (1.93)	120 (3)

σ_o -overburden pressure; S_{rm} – settlement rate in model dimension; ε_{max}- maximum total strain at the zone of maximum curvature; $(a/l)_{lim}$- limiting distortion level; d_c – Average crack depth; w_c – average crack width; Max $T_{g(mob)}$ – maximum mobilized tensile load of geogrid; * soil barrier is subjected to a maximum distortion level of 0.125; [a] not applicable; measured model values are given within the parenthesis.

Figure 2 shows the displacement profiles of the top surface of a 1.2 m thick soil barrier subjected to two different settlement rates for various stages of central settlements. A distinct variation in the displacement profiles can be noticed for various stages of central settlement. It can be observed that displacements have a maximum value at the mid-span of the soil barrier and tend to decrease significantly beyond the hinge axis (axis or line drawn on the position of mechanical hinge). The soil barrier subjected to two different settlement rates was found to experience almost identical deformation profiles at various stages of central settlements. However, the soil barrier subjected to slow settlement rate (S_{rm}= 0.5 mm/min) tends to deform slightly more compared to the relatively fast settlement rate (S_{rm} = 1 mm/min).

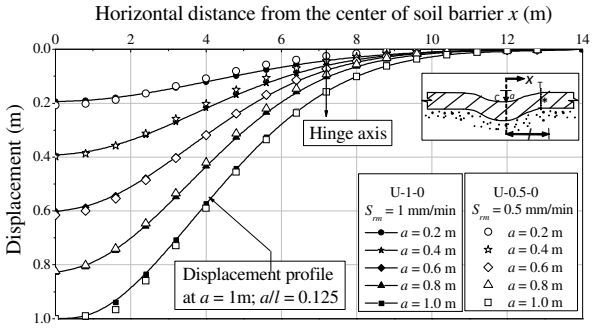

Figure 2 Displacement profiles measured at the top surface of the soil barrier tested at two different settlement ratios [Cases: U-1-0 and U-0.5-0]

The variation of total strain experienced by the soil barrier subjected to two different settlement rates along the horizontal distance from the centre of the soil barrier at various stages of central settlement is shown in Fig. 3. It can be observed that as the central settlement increases, the strain values also increase. Positive value of strain corresponds to tensile strain. A change of compressive strain to tensile strain can also be noticed along the length of both the soil barrier. The pattern of variation of strain distribution for both soil barriers was found to be almost identical. However, the soil barrier subjected to slow settlement rate (S_{rm}= 0.5 mm/min) tends to experience higher tensile strain irrespective of central settlement when compared to the relatively fast settlement rate (S_{rm} = 1 mm/min).

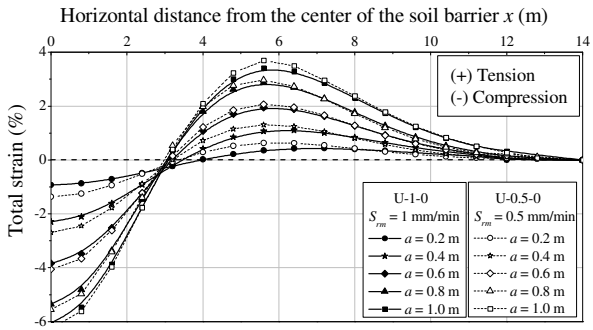

Figure 3 Variation in total strain with horizontal distance from the center of the soil barrier tested at two different settlement ratios [Cases: U-1-0 and U-0.5-0]

Figure 4 shows the variation of maximum total tensile strain at the zone of maximum curvature with settlement ratio and distortion level for various test cases. The strain values at various ranges of distortion level were found to be in the narrow bandwidth, for all soil barriers, tested at different settlement rates. A marginal delay in the occurrence of crack initiation and an increase in the strain value at crack initiation was noticed when the soil barrier was tested at slower settlement rate. When the total strain value increases beyond the permissible value of the soil barrier material, the probability of occurrence and propagation of the crack is inevitable and it can hamper the functionality of the landfill cover system. This can be witnessed from centrifuge tests as the induced strain levels are many times higher than the permissible tensile strain level of the soil barrier material.

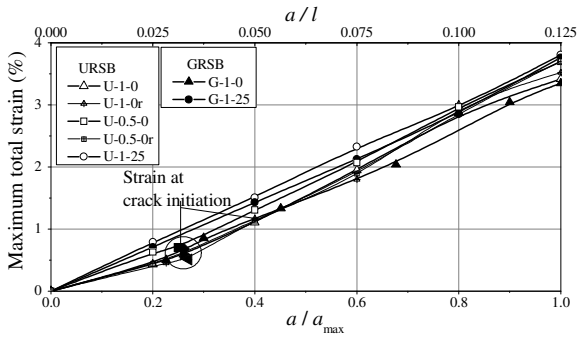

Figure 4 Variation of maximum total strain with a/a_{max} and a/l for various test cases

The status of the soil barrier before and after inducing central settlement of 1 m at a settlement rate of 1 mm/min is shown in Fig. 1a. Full-depth penetration of crack at the zone of maximum curvature can be noted. Figure 5 shows the status of soil barriers at the end of centrifuge test. It can be observed that for both settlement rates, cracks are formed at the zone of maximum curvature and extended throughout the breadth of the soil barrier. Multiple cracking patterns were observed for both the soil barrier with some cracks penetrating up to full-depth. Results from the repeatability tests (U-1-0r and U-0.5-0r) also show similar cracking pattern. This shows no significant variation in the cracking pattern when the soil barrier is tested at two different settlement rates.

The crack width along the width of the soil barrier was determined at various stages of central settlement using the image analysis of the digital photographs taken at the top surface markers. Average width of the crack w_c experienced by the soil barrier tested at two different settlement rates for various stages of central settlements are plotted against time in model and prototype dimensions, as shown in Fig. 6a. It can be observed that slope for the soil barrier subjected to a fastersettlement rate is steeper when compared to the soil barrier subjected to a slower settlementrate.

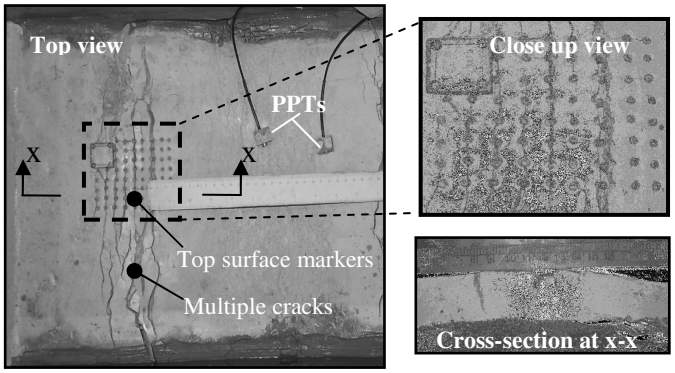

a) Case: U-1-0 (S_{rm} = 1 mm/min)

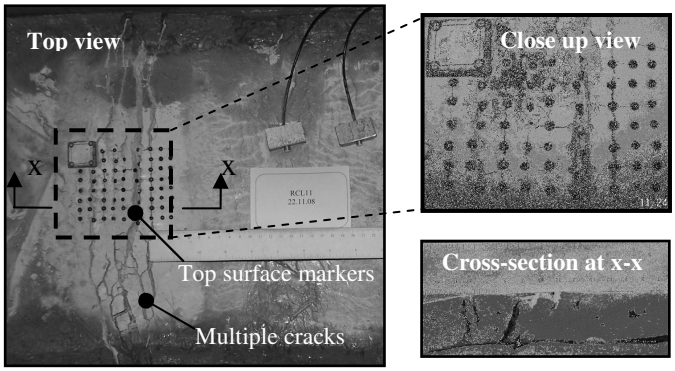

b) Case: U-0.5-0 (S_{rm} = 0.5 mm/min)

Figure 5 Status of unreinforced soil barriers subjected to two different settlement rates at the end of centrifuge test

Figure 6b shows the variation of infiltration ratio of the soil barrier tested at two different settlement rates with time (in model and prototype dimensions). It can be observed that the IFR for both soil barriers tested at two different settlement rates vary gently up to a certain value, followed by a steep variation. A lateral shift in curves can be noticed mainly because of the variation in the settlement rate. This figure also shows the repeatability of the test results.

Figure 7 shows the variation of average crack width in model and prototype dimensions against settlement ratio and distortion level. The variation of average crack width experienced by the soil barrier tested at two different settlement rates for various ranges of distortion level was to found to be almost identical and the magnitude of the maximum average crack width after inducing central settlement of 1 m was almost found to be equal.

When the IFR values are plotted against settlement ratio and distortion level for soil barriers tested at two different settlement rates, as shown in Fig. 8, a significant variation in the behavior can be noticed. In general, when the soil barrier is subjected to differential settlements, cracking was observed to initiate at a certain distortion level, followed by a widening of the cracks along lateral and vertical directions (along the depth of the soil barrier). When the width and depth of the cracks exceed certain limits, the water kept above the soil barrier tries to escape through the cracks. The distortion level corresponding to this condition is termed the limiting distortion level $(a/l)_{lim}$. Beyond this limiting distortion level, a steep variation of IFR occurs, which indicates the occurrence of water breakthrough of the soil barrier.

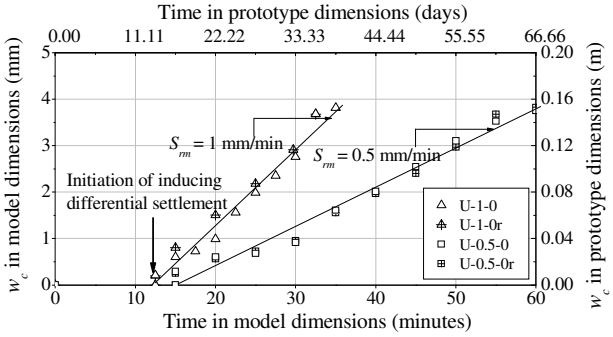

a) Variation of average crack width with time in model and prototype dimensions

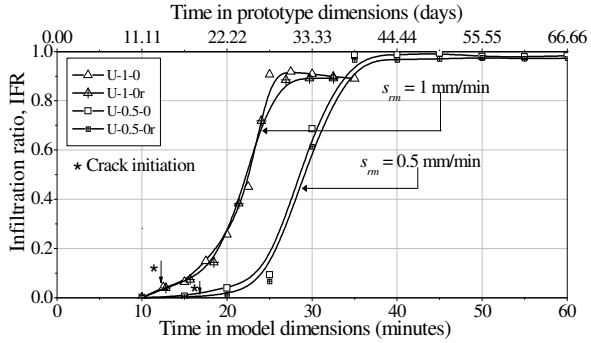

b) Variation of Infiltration ratio with time in model and prototype dimensions

Figure 6 Variation of average crack width and infiltration ratio with time for soil barriers tested at two different settlement rates

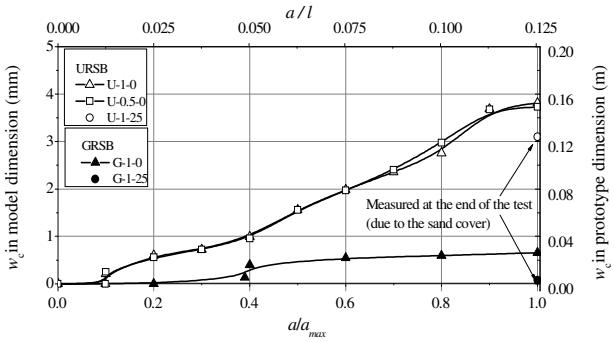

Figure 7 Variation of average crack width with settlement ratio and distortion level for various test cases

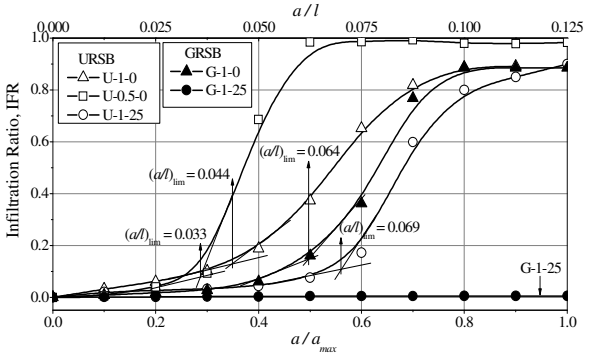

Figure 8 Variation of Infiltration ratio with settlement ratio and distortion level for various test cases
(Modified after Rajesh and Viswanadham, 2012)

From post-test examinations, it was confirmed that there is no side leakage for all the models, and reduction in volume of water is due to infiltration of the water either through pore spaces present in the soil barrier or through the crack formation. The limiting distortion level for the soil barrier tested at a slow settlement rate (S_{rm} = 0.5 mm/min) and relatively faster settlement rate (S_{rm} = 1 mm/min) was found to be 0.033 and 0.044 respectively. Even though the soil barrier tested at slower settlement rate has resisted slightly higher distortion at the onset of initiation of crack, limiting distortion level against water breakthrough was considerably lower. As the time involved for inducing particular central settlement/distortion level is higher for slow settlement rate when compared to faster settlement, the rate of depletion of water after initiation and propagation of cracks was found to be higher, hence limiting distortion level of soil barrier tested at slow settlement was found to be less.From literature (Richardson and Whitman, 1963; Nakase and Kamei, 1986), it was found that the undrained shear strength of the soil (compression as well as tension), especially for clayey soil, increases with an increase in the strain rate. Hence, reason behind an increase in the value of limiting distortion level at the higher settlement rate could be due to the relative increase in the tensile strength of the clay. However, this aspect needs further validation.The time taken for the initiation of cracking and the time taken from the initiation of cracking to the complete depletion of water for the slow settlement rate (28 days, in prototype dimensions) is almost twice that of the fast settlement rate (14 days, in prototype dimension). Hence, it can be inferred that the soil barrier subjected to a slow settlement rate can withstand its integrity for a long duration when compared to a faster settlement rate, even though the limiting distortion of the former barrier is less. From centrifuge tests, it can be concluded that when the induced distortion level in the field exceeds the limiting distortion level, the clay barrier tends to crack sufficiently enough to lose its integrity and fail to perform as an effective hydraulic barrier.

In the present study, the strengthening measure in the form of inclusion of geogrid reinforcement within the soil barrier was examined as an unreinforced soil barrier tend to loss its integrity at low distortion level itself. A centrifuge test was performed on a 1.2 m thick soil barrier reinforced with a instrumented model geogrid without any overburden pressure subjected to a settlement rate of 1 mm/min. When the soil barrier is reinforced with an instrumented model geogrid, maximum tensile strain experienced by the GRSB (Case: G-1-0) was found to be less compared to URSB (Case: U-1-0) (refer Fig. 4). A significant delay in the initiation of crack can be noticed with an inclusion of geogrid within the soil barrier. Figure 9a shows the crack pattern experienced by the soil barrier reinforced with geogrid after inducing a central settlement of 1 m. Average width and depth of cracks were found to reduce drastically with the inclusion of geogrid layer. Figure 7 shows the considerable reduction in the crack width at each and every stage of settlement ratio and distortion level. A significant delay in water breakthrough was observed with an inclusion of geogrid within the soil barrier, as shown in Fig. 8 (Cases: U-1-0 and G-1-0). The limiting distortion level was found to increase from 0.044 to 0.064 upon inclusion of geogrid within the soil barrier. The efficacy of geogrid reinforcement in restraining cracks, delay in water breakthrough, increase in limiting distortion level confirms the participation of geogrid in the load transfer mechanism and can be visually seen from the impression of ribs on the soil barrier at the location of model geogrid (Fig. 9a).

The mobilized tensile load distribution of geogrid while being subjected to distortion level can be determined from the results of calibrated strain gauge based instrumented geogrid. Figure 10 shows the maximum mobilized tensile load of geogrid at the zone of maximum curvature for various values of settlement ratio and distortion level. A steep increase in the maximum mobilized tensile load of geogrid was noticed up to a settlement ratio of 0.4 (i.e. a/l = 0.05) and thereafter a gentle increase was observed (Case: G-1-0). The initiation of the crack has occurred at a settlement ratio of 0.38 (Figs. 4, 7 and 8). This implies that the geogrid reinforcement layer tries to mobilize higher tensile load up to the initiation of crack, as soon as the soil barrier cracks, the load transfer from geogrid to soil gets reduced, hence reduction in the significant mobilization of tensile load. Nevertheless, the performance of GRSB was found to be many times superior than URSB

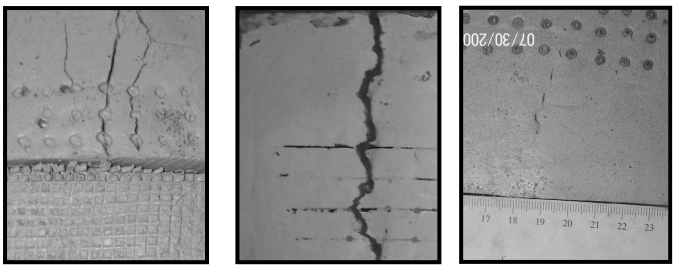

a) Case: G-1-0 b) Case: U-1-25 c) Case: G-1-25

Figure 9 Exposed portion of soil barriers (top view) at the end of the centrifuge test

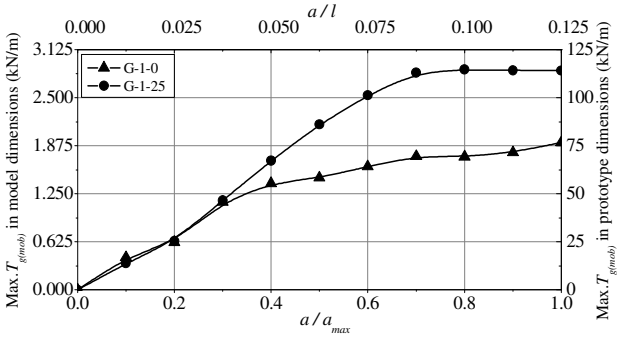

Figure 10 Variation of maximum mobilized tensile load at the zone of maximum curvature with settlement ratio and distortion level [Cases: G-1-0 and G-1-25]

4.2 Influence of overburden pressure

The influence of overburden pressure on the integrity of 1.2 m thick URSB and GRSB subjected to a settlement rate of 1 mm/min (in model dimensions) was studied by comparing tests with and without overburden pressure equivalent to that of a landfill cover system. The maximum tensile strain was found to increase with the provision of overburden pressure on both URSB and GRSB cases. When an overburden pressure of 25 kPa was applied to a URSB, change in cracking pattern from multiple cracks to single narrow crack can be noticed (Figs. 5a and 9b). From Table 4 and Fig. 7, it can be observed that the average crack width was found to reduce from 3.81 mm to 2.7 mm (in model dimension). However, both soil barriers were found to experience cracking extending up to full-depth of the soil barrier. The limiting distortion level was found to increase from 0.044 to 0.069 with the provision of overburden pressure (Fig. 8). When the soil barrier is reinforced with an instrumented model geogrid and subjected to an overburden pressure equivalent to that of cover system, crack free behavior with negligible infiltration even at a central settlement of 1 m (a/l = 0.125; a/a_{max} = 1) can be noticed (Figs. 1b and 9c). Figure 8 shows almost zero infiltration ratio up to a distortion level of 0.125, hence, the limiting distortion level for this GRSB case was reported as 0.125, which is the maximum possible distortion level that can be induced by the MDSS system. A slight reduction in the strain value was noticed upon inclusion of geogrid for various ranges of distortion level (Fig. 4). It can be noticed from Fig. 10 that the mobilization of maximum tensile load for an identical soil barrier with and without overburden pressure was found to be almost identical up to a/l = 0.038; thereafter the soil barrier with overburden pressure tends to mobilize higher tensile load in the geogrid. This implies that presence of overburden pressure enables the geogrid layer to mobilize higher tensile loads which could be

attributed to an increase in confinement stresses within the soil. This study reveals that the beneficial effect of the inclusion of geogrid reinforcement placed within the soil barrier to accomplish zero-infiltration barriers subjected to overburden pressures of 25 kPa.

5. CONCLUSIONS

In the present study, influence of settlement rate, geogrid reinforcement and overburden pressure on the deformation behavior of soil barriers was presented through centrifuge model tests conducted at 40g. Based on the analysis and interpretation of centrifuge test results, the following conclusions can be drawn:

1. Centrifuge test on 1.2 m thick un-reinforced soil barrier subjected to two different settlement rates (S_{rm} = 1 mm/min and 0.5 mm/min) without provision of any overburden pressure was found to experience multiple cracks, with few cracks extending up to the full-depth of the soil barrier. An identical cracking pattern and deformation profiles were noticed for both the soil barrier irrespective of settlement rate. A slight delay in the occurrence of crack initiation and an increase in the strain value at crack initiation was noticed when the soil barrier was tested at slower settlement rate. The limiting distortion level for the soil barrier tested at slow and fast settlement rate was found to be 0.033 and 0.044 respectively. Further, it can be inferred that the soil barrier subjected to a slow settlement rate can withstand its integrity for a long duration when compared to a faster settlement rate, even though the limiting distortion of the former barrier is less. From centrifuge tests, it can be concluded that when the induced distortion level in the field exceeds the limiting distortion level, the clay barrier tends to crack sufficiently enough to lose its integrity and fail to perform as an effective hydraulic barrier.
2. When the soil barrier was reinforced with a instrumented model geogrid tested at a settlement rate of 1 mm/min without provision of any overburden pressure, average width and depth of cracks were drastically reduced. A significant delay in the initiation of crack was observed upon inclusion of geogrid within the soil barrier. The limiting distortion level was observed to increase from 0.044 to 0.064. A steep increase in the maximum mobilized tensile load of geogrid was noticed up to a distortion level of 0.05 and thereafter a gentle increase was observed.
3. With the provision of overburden pressure equivalent to that of cover system, crack free barrier with negligible infiltration even at a distortion level of 0.125 was noticed. The mobilization of maximum tensile load for an identical soil barrier with and without overburden pressure was found to be almost identical up to a/l = 0.038; thereafter the soil barrier subjected to overburden pressure tends to mobilize higher tensile load in the geogrid. The maximum mobilized tensile load of model geogrid without any overburden pressure was found to be 77 kN/m. However, for identical conditions with the provision of overburden pressure it was increased to 120 kN/m. This implies that there is a requirement of mobilization of tensile load in the geogrid of the order of 120 kN/m in order to have a zero-infiltration barrier for a distortion level of 0.125.

6. ACKNOWLEDGEMENTS

The authors would like to thank Centrifuge staff at the National Geotechnical Centrifuge Facility of IIT Bombay for their untiring support throughout the present study.

7. REFERENCES

ASTM D 4595. (2005). "Standard test method for tensile properties of geotextiles by the wide-width strip method." Annual Book of ASTM Standards, Section 4, Vol. 04.13, Geosynthetics. ASTM, Philadelphia

Benson, C. H., Bralaz, M. A., Lane, D. T., and Rawe, J. M. (2007). "Practice of five bioreactor / recirculation landfills." Waste Management, Vol. 27(1), pp. 13-29.

Benson, C. H., Daniel, D. E., and Boutwell, G. P. (1999). "Field performance of compacted clay liners."J. Geotech. and Geoenvir. Engrg., ASCE, 125, Issue 5, pp. 391-403.

Daniel, D. E. (1993). "Geotechnical Practice for Waste Disposal." 1st Edition, Chapman & Hall, London.

Duplancic, N. (1990). "Landfill Deformation Monitoring and Stability Analysis." Geotechnics of Waste Fills - Theory and Practice, ASTM STP1070, Landva, A., and Knowles, G.D., Eds., American Society for Testing and Materials, Philadelphia, pp.303-314.

GRAM++. (2004). "Technical document." CSRE, Indian Institute of Technology Bombay.http://www.csre.iitb.ac.in/gram++/.

Gourc, J. P., Camp, S., Viswanadham, B. V.S., and Rajesh, S. (2010). "Deformation behaviour of clay cap barriers of hazardous waste containment systems: full-scale and centrifuge tests." Geotextiles and Geomembranes, 28, Issue 3, pp. 281-291.

Jessberger, H. L., and Stone, K. J. L. (1991). "Subsidence effect on clay barriers." Geotechnique, 41, Issue 2, pp. 185–194.

Koerner, R. M., and Daniel, D. E. (1997). "Final covers for solid waste landfills and abandoned dumps." ASCE Press, New York, pp. 256.

Kuo Ch.M., and Hsu T.R. (2003). "Traffic induced reflective cracking on pavements with geogrid reinforced asphalt concrete overlay." Annual meeting of the Transportation Research Board, CD-ROM, Transportation Research Board, Washington, D.C, pp. 1–23.

Nakase, A., and Kamei, T. (1986). "Influence of strain rate on undrained shear characteristics of ko- consolidation cohesive soils." Soils and Foundations, 26, Issue 1, pp. 85-95.

Qian, X., Koerner, R. M., and Gray, D. H. (2002). "Geotechnical aspects of landfill design and construction." Prentice Hall, New Jersey, USA, pp. 431-436.

Rajesh, S., and Viswanadham, B.V.S. (2009). "Evaluation of geogrid as a reinforcement layer in clay based engineered barriers." Applied Clay Science, 46, Issue 2, pp.153-165.

Rajesh, S., and Viswanadham, B.V.S. (2010). "Development of a Motor-based differential settlement simulator setup for a Geotechnical Centrifuge." Geotechnical Testing Journal, ASTM, 33, Issue 6, pp. 507-513.

Rajesh, S., and Viswanadham, B.V.S. (2012). "Modelling and instrumentation of geogrid reinforced soil barriers of landfill covers."J. Geotech. and Geoenvir. Engrg., ASCE, 138, Issue 1, pp. 26-37.

Richardson, A. M., and Whitman, R. V. (1963). "Effect of strain rate upon undrained shear resistance of a saturated remoulded fat clay." Geotechnique, Vol. 13 (3), pp. 310-324.

Schofield, A. N. (1980). "Cambridge geotechnical centrifuge operations." Geotechnique, 30, Issue 3, pp. 227–268.

Tognon, A. R., Rowe, R. K., and Moore, I.D. (2000). "Geomembrane strain observed in large-scale testing of protection layers."J. Geotech. and Geoenvir. Engrg., ASCE,126, Issue 12, pp. 1194-1208.

Viswanadham, B. V. S., and König, D. (2004). "Studies on scaling and instrumentation of a geogrid." Geotextiles and Geomembranes, 22, Issue 5, pp. 307-328.

Viswanadham, B. V. S., and Mahesh, K. V. (2002). "Modelling deformation behaviour of clay liners in a small centrifuge."Can. Geotech. J., 39, Issue 6, pp. 1406-1418.

Viswanadham, B. V. S. and Jessberger, H. L. (2005). "Centrifuge modeling of geosynthetic reinforced clay liners of landfills". J. Geotech. and Geoenvir. Engrg., ASCE, 131, Issue 5, pp 564-574.

Viswanadham, B. V. S., and Rajesh, S. (2009). "Centrifuge model test on clay based engineered barriers subjected to differential settlement." Applied Clay Science, 42, Issues 3-4, pp. 460-472.

Viswanadham, B.V.S., Rajesh, S., Divya, P.V., and Gourc, J.P. (2011). "Influence of randomly distributed geofibers on the integrity of clay-based landfill covers." Geosynthetic International, 18, Issue 5, pp. 255-271.